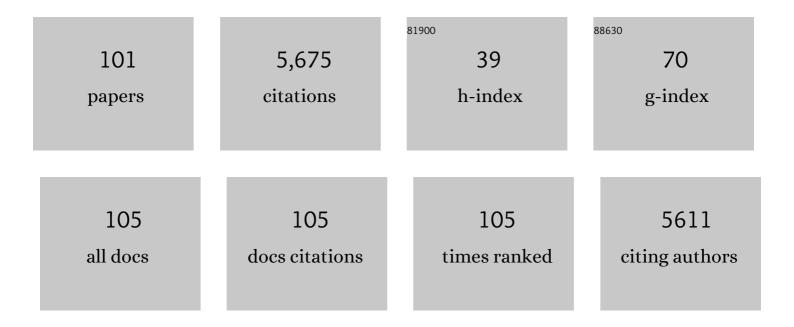
Sabine Kasten

List of Publications by Year in descending order

Source: https://exaly.com/author-pdf/1174582/publications.pdf Version: 2024-02-01



#	Article	IF	CITATIONS
1	Crystalline iron oxides stimulate methanogenic benzoate degradation in marine sediment-derived enrichment cultures. ISME Journal, 2021, 15, 965-980.	9.8	25
2	Dropstones in the Mar del Plata Canyon Area (SW Atlantic): Evidence for Provenance, Transport, Distribution, and Oceanographic Implications. Geochemistry, Geophysics, Geosystems, 2021, 22, e2020GC009333.	2.5	7
3	Electron Acceptor Availability Shapes Anaerobically Methane Oxidizing Archaea (ANME) Communities in South Georgia Sediments. Frontiers in Microbiology, 2021, 12, 617280.	3.5	11
4	Iron and sulfate reduction structure microbial communities in (sub-)Antarctic sediments. ISME Journal, 2021, 15, 3587-3604.	9.8	29
5	Evolution of (Bioâ€)Geochemical Processes and Diagenetic Alteration of Sediments Along the Tectonic Migration of Ocean Floor in the Shikoku Basin off Japan. Geochemistry, Geophysics, Geosystems, 2021, 22, e2020GC009585.	2.5	11
6	New insights into large-scale trends of apparent organic matter reactivity in marine sediments and patterns of benthic carbon transformation. Biogeosciences, 2021, 18, 4651-4679.	3.3	19
7	Geochemical consequences of oxygen diffusion from the oceanic crust into overlying sediments and its significance for biogeochemical cycles based on sediments of the northeast Pacific. Biogeosciences, 2021, 18, 4965-4984.	3.3	6
8	Early diagenesis of sulfur in Bornholm Basin sediments: The role of upward diffusion of isotopically "heavy―sulfide. Geochimica Et Cosmochimica Acta, 2021, 313, 359-377.	3.9	7
9	Impact of Upward Oxygen Diffusion From the Oceanic Crust on the Magnetostratigraphy and Iron Biomineralization of East Pacific Ridge-Flank Sediments. Frontiers in Earth Science, 2021, 9, .	1.8	1
10	Post-depositional manganese mobilization during the last glacial period in sediments of the eastern Clarion-Clipperton Zone, Pacific Ocean. Earth and Planetary Science Letters, 2020, 532, 116012.	4.4	13
11	A prominent isotopic fingerprint of nitrogen uptake by anaerobic methanotrophic archaea. Chemical Geology, 2020, 558, 119972.	3.3	13
12	Impact of iron release by volcanic ash alteration on carbon cycling in sediments of the northern Hikurangi margin. Earth and Planetary Science Letters, 2020, 541, 116288.	4.4	15
13	Constraining the Age and Evolution of the Tuaheni Landslide Complex, Hikurangi Margin, New Zealand, Using Poreâ€Water Geochemistry and Numerical Modeling. Geophysical Research Letters, 2020, 47, e2020GL087243.	4.0	9
14	Discovery of a giant cold-water coral mound province along the northern Argentine margin and its link to the regional Contourite Depositional System and oceanographic setting. Marine Geology, 2020, 427, 106223.	2.1	22
15	Early diagenesis of iron and sulfur in Bornholm Basin sediments: The role of near-surface pyrite formation. Geochimica Et Cosmochimica Acta, 2020, 284, 43-60.	3.9	33
16	Impact of small-scale disturbances on geochemical conditions, biogeochemical processes and element fluxes in surface sediments of the eastern Clarion–Clipperton Zone, Pacific Ocean. Biogeosciences, 2020, 17, 1113-1131.	3.3	18
17	Calcium phosphate control of REY patterns of siliceous-ooze-rich deep-sea sediments from the central equatorial Pacific. Geochimica Et Cosmochimica Acta, 2019, 251, 56-72.	3.9	42
18	Sources of laminated sediments in the northeastern Arabian Sea off Pakistan and implications for sediment transport mechanisms during the late Holocene. Holocene, 2019, 29, 130-144.	1.7	7

#	Article	IF	CITATIONS
19	Rates and Microbial Players of Iron-Driven Anaerobic Oxidation of Methane in Methanic Marine Sediments. Frontiers in Microbiology, 2019, 10, 3041.	3.5	51
20	Stromatolites below the photic zone in the northern Arabian Sea formed by calcifying chemotrophic microbial mats. Geology, 2018, 46, 339-342.	4.4	33
21	The geochemical behavior of metals during early diagenetic alteration of buried manganese nodules. Deep-Sea Research Part I: Oceanographic Research Papers, 2018, 142, 16-33.	1.4	47
22	Temperature Controls Crystalline Iron Oxide Utilization by Microbial Communities in Methanic Ferruginous Marine Sediment Incubations. Frontiers in Microbiology, 2018, 9, 2574.	3.5	23
23	Phosphorus dynamics around the sulphate-methane transition in continental margin sediments: Authigenic apatite and Fe(II) phosphates. Marine Geology, 2018, 404, 84-96.	2.1	45
24	Biogeochemical Regeneration of a Nodule Mining Disturbance Site: Trace Metals, DOC and Amino Acids in Deep-Sea Sediments and Pore Waters. Frontiers in Marine Science, 2018, 5, .	2.5	27
25	Iron cycling and stable Fe isotope fractionation in Antarctic shelf sediments, King George Island. Geochimica Et Cosmochimica Acta, 2018, 237, 320-338.	3.9	38
26	Natural spatial variability of depositional conditions, biogeochemical processes and element fluxes in sediments of the eastern Clarion-Clipperton Zone, Pacific Ocean. Deep-Sea Research Part I: Oceanographic Research Papers, 2018, 140, 159-172.	1.4	86
27	Iron oxide reduction in methane-rich deep Baltic Sea sediments. Geochimica Et Cosmochimica Acta, 2017, 207, 256-276.	3.9	95
28	Evidence for a palaeo-subglacial lake on the Antarctic continental shelf. Nature Communications, 2017, 8, 15591.	12.8	32
29	Sulfur Cycling in an Iron Oxide-Dominated, Dynamic Marine Depositional System: The Argentine Continental Margin. Frontiers in Earth Science, 2017, 5, .	1.8	70
30	Widespread seawater circulation in 18–22 Ma oceanic crust: Impact on heat flow and sediment geochemistry. Geology, 2017, 45, 799-802.	4.4	37
31	Carbon cycling fed by methane seepage at the shallow Cumberland Bay, South Georgia, subâ€Antarctic. Geochemistry, Geophysics, Geosystems, 2016, 17, 1401-1418.	2.5	23
32	Quantifying manganese and nitrogen cycle coupling in manganeseâ€rich, organic carbonâ€starved marine sediments: Examples from the Clarion lipperton fracture zone. Geophysical Research Letters, 2016, 43, 7114-7123.	4.0	41
33	Diffusive transfer of oxygen from seamount basaltic crust into overlying sediments: An example from the Clarion–Clipperton Fracture Zone. Earth and Planetary Science Letters, 2016, 433, 215-225.	4.4	36
34	Mössbauer spectroscopy and X-ray fluorescence studies on sediments from the methanic zone of the Helgoland mud area, North Sea. Hyperfine Interactions, 2016, 237, 1.	0.5	0
35	Cyclic magnetite dissolution in Pleistocene sediments of the abyssal northwest Pacific Ocean: Evidence for glacial oxygen depletion and carbon trapping. Pale ceanography, 2016, 31, 600-624. Mg/Ca- <mmil:math <="" altimg="sil.gif" ns:mml="http://www.W3.org/1998/Math/Math/MathME" td="" xm=""><td>3.0</td><td>53</td></mmil:math>	3.0	53
36	overflow="scroll"> <mml:mi mathvariant="normal">{"</mml:mi> <mml:msubsup><mml:mrow><mml:mi mathvariant="normal">CO</mml:mi </mml:mrow><mml:mrow><mml:mn>3</mml:mn><mml:mspace width="0.25em" /><mml:mtext>pore</mml:mtext><mml:mspace <br="" width="0.25em">/><mml:mtext>water</mml:mtext></mml:mspace></mml:mspace </mml:mrow><mml:mn>2</mml:mn><mml:mo>â^'</mml:mo>< calibration for Globobulimina spp.: A sensitive paleot. Earth and Planetary Science Letters, 2016, 438, 95</mml:msubsup>	4.4 /mml:mro	20 w>

#	Article	IF	CITATIONS
37	Determination of the stable iron isotopic composition of sequentially leached iron phases in marine sediments. Chemical Geology, 2016, 421, 93-102.	3.3	58
38	Timing and structure of Mega ACZ events during Heinrich Stadial 1. Geophysical Research Letters, 2015, 42, 5477.	4.0	93
39	Microbial Communities and Organic Matter Composition in Surface and Subsurface Sediments of the Helgoland Mud Area, North Sea. Frontiers in Microbiology, 2015, 6, 1290.	3.5	102
40	Distinct microbial populations are tightly linked to the profile of dissolved iron in the methanic sediments of the Helgoland mud area, North Sea. Frontiers in Microbiology, 2015, 06, 365.	3.5	72
41	A continental-weathering control on orbitally driven redox-nutrient cycling during Cretaceous Oceanic Anoxic Event 2. Geology, 2015, 43, 963-966.	4.4	77
42	Constraining silica diagenesis in methane-seep deposits. Palaeogeography, Palaeoclimatology, Palaeoecology, 2015, 420, 13-26.	2.3	30
43	An inorganic geochemical argument for coupled anaerobic oxidation of methane and iron reduction in marine sediments. Geobiology, 2014, 12, 172-181.	2.4	180
44	Global rates of marine sulfate reduction and implications for sub–sea-floor metabolic activities. Science, 2014, 344, 889-891.	12.6	253
45	Impact of depositional and biogeochemical processes on small scale variations in nodule abundance in the Clarionâ€Clipperton Fracture Zone. Deep-Sea Research Part I: Oceanographic Research Papers, 2014, 91, 125-141.	1.4	113
46	First evidence of widespread active methane seepage in the Southern Ocean, off the sub-Antarctic island of South Georgia. Earth and Planetary Science Letters, 2014, 403, 166-177.	4.4	40
47	Subduction zone earthquake as potential trigger of submarine hydrocarbon seepage. Nature Geoscience, 2013, 6, 647-651.	12.9	105
48	Impact of Indus River discharge on productivity and preservation of organic carbon in the Arabian Sea over the twentieth century. Geology, 2012, 40, 399-402.	4.4	13
49	Gas hydrate decomposition recorded by authigenic barite at pockmark sites of the northern Congo Fan. Geo-Marine Letters, 2012, 32, 515-524.	1.1	25
50	A comparison of mm scale resolution techniques for element analysis in sediment cores. Journal of Analytical Atomic Spectrometry, 2012, 27, 1574.	3.0	23
51	Geochemical distribution patterns as indicators for productivity and terrigenous input off NW Africa. Deep-Sea Research Part I: Oceanographic Research Papers, 2012, 66, 51-66.	1.4	24
52	Diagenetic barium cycling in Black Sea sediments – A case study for anoxic marine environments. Geochimica Et Cosmochimica Acta, 2012, 88, 88-105.	3.9	67
53	Influence of diagenesis on the stable isotopic composition of biogenic carbonates from the Gulf of Tehuantepec oxygen minimum zone. Geochemistry, Geophysics, Geosystems, 2012, 13, .	2.5	16
54	Bacterial diversity and biogeochemistry of different chemosynthetic habitats of the REGAB cold seep (West African margin, 3160 m water depth). Biogeosciences, 2012, 9, 5031-5048.	3.3	43

#	Article	lF	CITATIONS
55	The effect of meter-scale lateral oxygen gradients at the sediment-water interface on selected organic matter based alteration, productivity and temperature proxies. Biogeosciences, 2012, 9, 1553-1570.	3.3	32
56	Interaction between hydrocarbon seepage, chemosynthetic communities, and bottom water redox at cold seeps of the Makran accretionary prism: insights from habitat-specific pore water sampling and modeling. Biogeosciences, 2012, 9, 2013-2031.	3.3	87
57	Pore Water Geochemistry as a Tool for Identifying and Dating Recent Mass-Transport Deposits. , 2012, , 87-97.		5
58	Distribution and abundance of gas hydrates in near-surface deposits of the HÃ¥kon Mosby Mud Volcano, SW Barents Sea. Geochemistry, Geophysics, Geosystems, 2011, 12, n/a-n/a.	2.5	29
59	An interdisciplinary investigation of a recent submarine mass transport deposit at the continental margin off Uruguay. Geochemistry, Geophysics, Geosystems, 2011, 12, n/a-n/a.	2.5	32
60	Petroleum degradation and associated microbial signatures at the Chapopote asphalt volcano, Southern Gulf of Mexico. Geochimica Et Cosmochimica Acta, 2011, 75, 4377-4398.	3.9	41
61	Reconstructing changes in seep activity by means of pore water and solid phase Sr/Ca and Mg/Ca ratios in pockmark sediments of the Northern Congo Fan. Marine Geology, 2011, 287, 1-13.	2.1	119
62	Pore Waters. Encyclopedia of Earth Sciences Series, 2011, , 742-746.	0.1	0
63	Oxidative sulfur cycling in the deep biosphere of the Nankai Trough, Japan. Geology, 2010, 38, 851-854.	4.4	33
64	Gas hydrates in shallow deposits of the Amsterdam mud volcano, Anaximander Mountains, Northeastern Mediterranean Sea. Geo-Marine Letters, 2010, 30, 187-206.	1.1	56
65	Selective preservation of organic matter in marine environments; processes and impact on the sedimentary record. Biogeosciences, 2010, 7, 483-511.	3.3	331
66	Biogeochemistry of a low-activity cold seep in the Larsen B area, western Weddell Sea, Antarctica. Biogeosciences, 2009, 6, 2383-2395.	3.3	58
67	A late Miocene–early Pliocene Antarctic deepwater record of repeated iron reduction events. Marine Geology, 2009, 266, 198-211.	2.1	9
68	Are the Kimmeridge Clay deposits affected by "burn-down―events? Palynological and geochemical studies on a 1 metre long section from the Upper Kimmeridge Clay Formation (Dorset, UK). Sedimentary Geology, 2009, 222, 301-313.	2.1	4
69	Biogeochemical controls on authigenic carbonate formation at the Chapopote "asphalt volcanoâ€; Bay of Campeche. Chemical Geology, 2009, 266, 390-402.	3.3	52
70	Euphotic zone bacterioplankton sources major sedimentary bacteriohopanepolyols in the Holocene Black Sea. Geochimica Et Cosmochimica Acta, 2009, 73, 750-766.	3.9	38
71	Geochemical environment of the Coniacian–Santonian western tropical Atlantic at Demerara Rise. Palaeogeography, Palaeoclimatology, Palaeoecology, 2009, 273, 286-301.	2.3	26
72	Chapter 1 Impacts of the Oceans on Climate Change. Advances in Marine Biology, 2009, 56, 1-150.	1.4	110

#	Article	IF	CITATIONS
73	Pockmarks in the Northern Congo Fan area, SW Africa: Complex seafloor features shaped by fluid flow. Marine Geology, 2008, 249, 206-225.	2.1	95
74	Diagenetic changes of magnetic and geochemical signals by anaerobic methane oxidation in sediments of the Zambezi deep-sea fan (SW Indian Ocean). Marine Geology, 2008, 255, 118-130.	2.1	116
75	A novel, multiâ€layered methanotrophic microbial mat system growing on the sediment of the Black Sea. Environmental Microbiology, 2008, 10, 1934-1947.	3.8	55
76	Rock magnetic identification and geochemical process models of greigite formation in Quaternary marine sediments from the Gulf of Mexico (IODP Hole U1319A). Earth and Planetary Science Letters, 2008, 275, 233-245.	4.4	100
77	Redox sensitivity of P cycling during marine black shale formation: Dynamics of sulfidic and anoxic, non-sulfidic bottom waters. Geochimica Et Cosmochimica Acta, 2008, 72, 3703-3717.	3.9	196
78	The Impacts of the Oceans on Climate Change. , 2008, , .		1
79	Sources and modes of terrigenous sediment input to the Chilean continental slope. Quaternary International, 2007, 161, 67-76.	1.5	36
80	Barium in sediments off northwest Africa: A tracer for paleoproductivity or meltwater events?. Paleoceanography, 2006, 21, n/a-n/a.	3.0	32
81	Active and buried authigenic barite fronts in sediments from the Eastern Cape Basin. Earth and Planetary Science Letters, 2006, 241, 876-887.	4.4	114
82	Sulfur Cycling and Methane Oxidation. , 2006, , 271-309.		159
83	Diagenetic Alteration of Magnetic Signals by Anaerobic Oxidation of Methane Related to a Change in Sedimentation Rate. Geochimica Et Cosmochimica Acta, 2005, 69, 4117-4126.	3.9	144
84	Different nutrient sources forcing increased productivity during eastern Mediterranean S1 sapropel formation as reflected by calcareous dinoflagellate cysts. Paleoceanography, 2004, 19, n/a-n/a.	3.0	31
85	A combined geochemical and rock-magnetic investigation of a redox horizon at the last glacial/interglacial transition. Physics and Chemistry of the Earth, 2004, 29, 921-931.	2.9	22
86	Control of sulfate pore-water profiles by sedimentary events and the significance of anaerobic oxidation of methane for the burial of sulfur in marine sediments. Geochimica Et Cosmochimica Acta, 2003, 67, 2631-2647.	3.9	220
87	Processes and Signals of Nonsteady-State Diagenesis in Deep-Sea Sediments and their Pore Waters. , 2003, , 431-459.		41
88	Late Quaternary Sedimentation and Early Diagenesis in the Equatorial Atlantic Ocean: Patterns, Trends and Processes Deduced from Rock Magnetic and Geochemical Records. , 2003, , 461-497.		10
89	North Atlantic Deep Water export to the Southern Ocean over the past 14 Myr: Evidence from Nd and Pb isotopes in ferromanganese crusts. Paleoceanography, 2002, 17, 12-1-12-9.	3.0	129
90	Barium peaks at glacial terminations in sediments of the equatorial Atlantic Ocean—relicts of deglacial productivity pulses?. Chemical Geology, 2001, 175, 635-651.	3.3	60

#	Article	IF	CITATIONS
91	Reconstruction of primary productivity from the barium contents in surface sediments of the South Atlantic Ocean. Marine Geology, 2001, 177, 13-24.	2.1	58
92	Computer simulation of deep sulfate reduction in sediments of the Amazon Fan. International Journal of Earth Sciences, 2000, 88, 641-654.	1.8	29
93	Sulfate Reduction in Marine Sediments. , 2000, , 263-281.		51
94	Biogenic Barium as a Proxy for Paleoproductivity: Methods and Limitations of Application. , 1999, , 345-364.		37
95	Rare earth elements in manganese nodules from the South Atlantic Ocean as indicators of oceanic bottom water flow. Marine Geology, 1998, 146, 33-52.	2.1	36
96	Deep Sulfate Reduction Completely Mediated by Anaerobic Methane Oxidation in Sediments of the Upwelling Area off Namibia. Geochimica Et Cosmochimica Acta, 1998, 62, 455-464.	3.9	286
97	Simultaneous formation of iron-rich layers at different redox boundaries in sediments of the Amazon deep-sea fan. Geochimica Et Cosmochimica Acta, 1998, 62, 2253-2264.	3.9	120
98	Solid-phase manganese in Southeast Atlantic sediments: Implications for the paleoenvironment. Marine Geology, 1994, 121, 317-332.	2.1	39
99	Data report: solid-phase major and minor elements and iron and sulfur species in sediments of the Anholt Basin, Baltic Sea collected during IODP Expedition 347. Proceedings of the Integrated Ocean Drilling Program Integrated Ocean Drilling Program, 0, , .	1.0	Ο
100	Benthic Carbon Remineralization and Iron Cycling in Relation to Sea Ice Cover along the Eastern Continental Shelf of the Antarctic Peninsula. Journal of Geophysical Research: Oceans, 0, , .	2.6	5
101	Editorial: Advances in Microbial Iron Cycling. Frontiers in Microbiology, 0, 13, .	3.5	0